Solubilization of carbon nanoparticles, nanotubes, nano-onions, and nanodiamonds through covalent functionalization with sucrose

*O. V. Kuznetsov,[a] M. X. Pulikkathara,[b] R. F. M. Lobo,[c] and V. N. Khabashesku[a,d]**

[a]*Department of Physics and Astronomy, Rice University, Houston, 77005 Texas, USA*
[b]*Department of Chemistry, Rice University, Houston, 77005 Texas, USA*
[c]*Department of Physics, Faculty of Sciences and Technology, New University of Lisbon, Caparica, Portugal; Group for Nanoscale Science and Technology (GNCN/FCT—ICEMS/IST), Av. Rovisco Pais, 1001 Lisbon, Portugal*
[d]*Department of Chemical and Biomolecular Engineering, University of Houston, 77204 Houston, Texas, USA*
Fax: (713) 743 8955. E-mail valery@uh.edu

Water solubilization of carbon nanoparticles (nanocarbons), single-walled nanotubes (SWCNTs), nano-onions (NOs) and nanodiamonds (NDs) has been achieved through their covalent functionalization by fluorination and subsequent derivatization with sucrose. The covalent bonding of sucrose to the surface of the fluorinated nanocarbons was attained by a one-step fluorine substitution reaction with sucrose-derived lithium monosucrate under sonication in DMF at room temperature. This chemical process provides a simple, inexpensive, and easily scalable method for hydrophilic chemical modification of SWCNT, NO, and ND surfaces to produce sucrose-functionalized nanocarbons that become soluble in water, DMF, ethanol, and other polar solvents. The sucrose-functionalized nanocarbon particles are expected to be biocompatible due to the abundance of hydroxyl groups available for hydrogen bonding and further chemical modification. Relevant examples have been given.

Key words: nanocarbon materials, carbon nanotubes, nanodiamond, functionalization, solubilization.

Single-walled carbon nanotubes (SWCNTs), nano-onions (NOs), and nanodiamond (ND) particles possess extraordinary mechanical, electronic, thermal, and tribological properties. They have significant potential for use as components for design of new functional materials and devices.[1–7] The development of methods for solubilization of nanoparticles is essential to make feasible their application in polymer composites, coatings, ceramics, and biomaterials. Specifically, water-soluble carbon nanomaterials have attracted much recent attention for a number of biomedical applications, including biosensing and drug delivery.[8] However, most of the previous work on water solubilization of carbon nanostructures was based upon surface activation through strong oxidizing acid treatment followed by several-step derivatization and coupling reactions[8–10] which utilize expensive polyethylene glycol (PEG)-derived coupling reagents.[8,11] In particular, the most recently developed methods for solubilization of carbon nanotubes require severe oleum functionalization conditions,[11,12] which cause the sidewall etching and degradation of mechanical strength of the nanotube. For these reasons, finding functionalization routes for carbon nanoparticles which can utilize mild reaction conditions and inexpensive reagents is important. It is expected that organic molecules possessing the terminal carboxyl, amide, hydroxyl, and other hydrophilic moieties can serve as the reagents of choice in these studies.

Fluorination is a powerful tool for surface modification of carbon nanoparticles and therefore this process is extensively studied, particularly for carbon nanotubes.[13–15] Our previous studies have shown that fluoronanotubes (F-SWCNTs)[13a,14b,15] and fluoronanodiamonds (F-NDs)[16] can be used as convenient precursors for subsequent derivatizations through displacement of fluorine in the C—F bonds by strong nucleophiles. The reactions of F-SWCNTs and F-NDs with amino acids and urea have yielded nanocarbon derivatives with terminal carboxyl and amide moieties which formed relatively stable colloidal suspension solutions in water.[16–19] SWCNTs with covalently attached hydroxyl-terminated functional groups

Published in Russian in *Izvestiya Akademii Nauk. Seriya Khimicheskaya,* No. 8, pp. 1462—1472, August, 2010.
1066-5285/10/5908-1495

Scheme 1

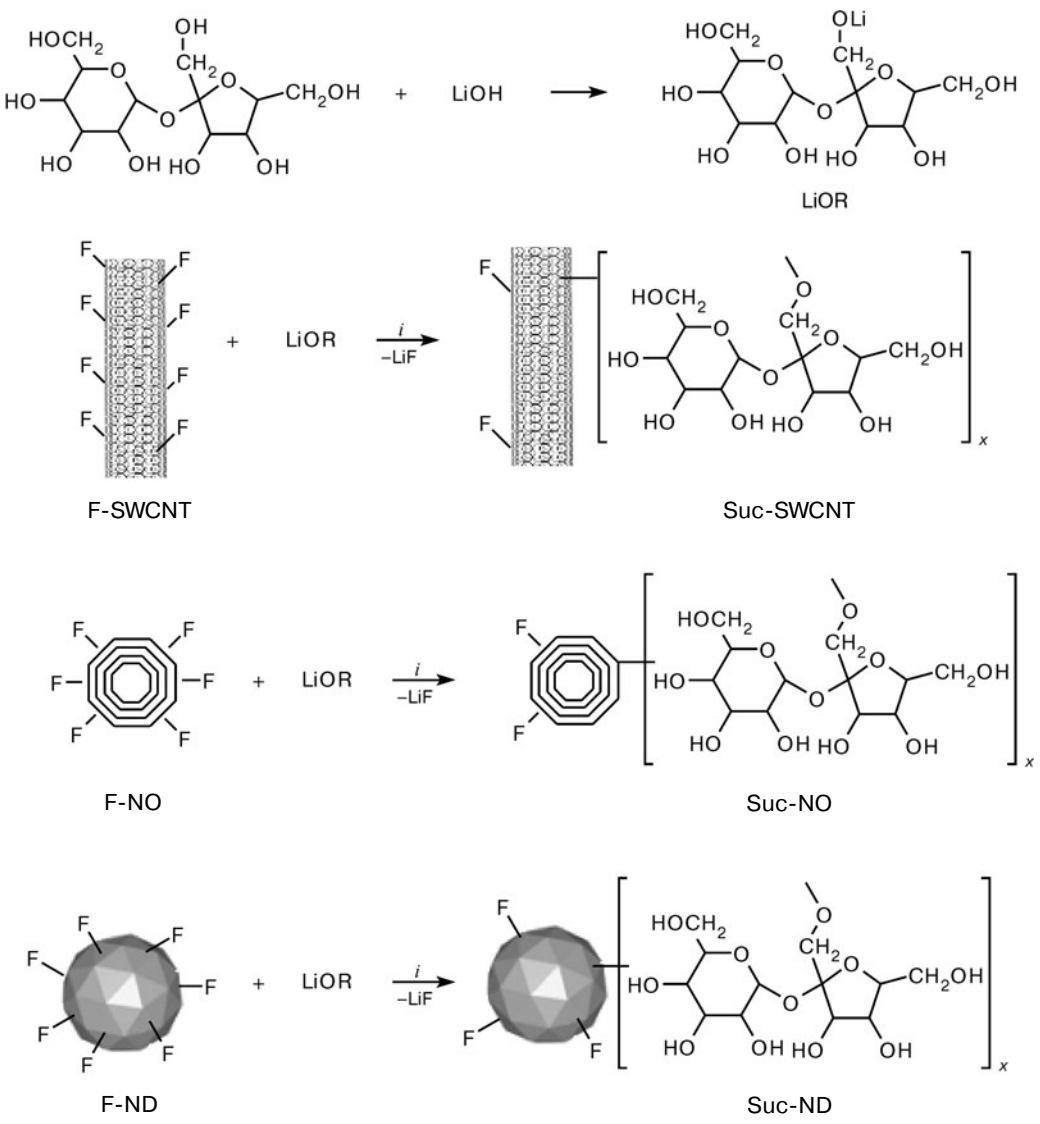

i. Sonication, DMF

have also been prepared through substitution of fluorine in F-SWCNTs by monoalkoxides derived from diols and glycerol.[20] The "hydroxyl-SWCNTs" produced by this method are soluble in water. However, their solubility is not higher than 40 mg L^{-1} and their precipitation from solutions is observed in less than a week. Nevertheless, the results of this early work[20] suggest that an increase in the number of free hydroxyl groups in the side chain of each molecule covalently attached to the surface of a carbon nanoparticle should assist in enhancement of water solubility. For that reason, we have chosen for the present study a polyol-type reagent, such as sucrose, because it contains as many as eight hydroxyl groups per molecule, is highly soluble in water, and is inexpensive. Sucrose is also of biomedical importance as a carbohydrate playing an important role in human nutrition and health.

The lithium monosucrate derivative, generated from sucrose through a treatment with lithium hydroxide, has been reacted with fluorinated nanocarbons (F-SWCNTs, F-NOs, and F-NDs) used as precursors in the C—F bond substitution reactions (Scheme 1). As a result of these reactions, sucrose functionalized carbon nanotubes (Suc-SWCNTs), nano-onions (Suc-NOs), and nanodiamonds (Suc-ND) were produced in a simple one-step process. These particles showed enhanced water solubility and were expected to be biocompatible. Besides the biomedical field, these functionalized carbon nanostructures are expected to find applications in mechanically reinforced composites[21,22] due to improved interfacial interaction and dispersion in

polymers, ceramics, and cements being enabled by sucrose functional groups and their subsequent derivatization.

Experimental

F-SWCNTs were obtained from Carbon Nanotechnology Inc. (at present Unidym) where they have been produced by fluorination of SWCNTs with F_2 gas at 150 °C.[13a] SWCNTs have been synthesized through a HipCO process originally invented at Rice University[23a] and then commercialized by Carbon Nanotechnology Inc. An XPS analysis of the F-SWCNTs done on at least five spots of the sample yielded an average C_2F stoichiometry for this fluorocarbon. Electron probe microanalysis of the TGA solid residue yielded about 0.2 at.% Fe content in the F-SWCNTs. Atomic force microscopy (AFM) analysis has shown that relatively short tubes with length distribution in the range of 200—700 nm and an average diameter of about 1.3 nm make up more than 90% of F-SWCNTs. The carbon nano-onions used in the present work were received in a powder form. The NO powder was synthesized from carbon black by a proprietary inductive heating batch method that produces very high purity material in large quantities with NO diameters ranging from 30 to 100 nm.[23b] Nanodiamond powder produced by detonation method was purchased from Nanostructured and Amorphous Materials Inc. (Houston). The phase purity of the ND powder was higher than 97% (less than 2.5% of graphite and amorphous carbon, 0.1—0.15% Fe, 0.1—0.3% Si) with the particle sizes ranging from 3.5 to 6.5 nm. The NO and ND powders were fluorinated with a fluorine (10%)-helium (90%) gas mixture purchased from Spectra Gases.

The fluorination of nanocarbon powders was carried out in a custom-built fluorination apparatus described elsewhere.[13] Direct fluorination was used to attach fluorine atoms to the surface of NO and ND particles at reaction temperatures of 350 °C and 310 °C, respectively, by following a previously developed procedure.[7,16] The fluorine content in the fluorinated NO and ND (F-NO and F-ND) powders was 44.2 and 14.0 at. %, respectively, according to XPS analysis (Table 1).

Sucrose functionalization of all fluorinated carbon nanostructures was carried out using the same procedure. First, 50 mg of F-SWCNTs (F-NOs, F-NDs) was dispersed in DMF by sonication in a 100 W bath sonicator for 90 min to obtain a suspension having approximately 1 mg mL^{-1} concentration. In a separate vial, a lithium monosucrate LiOR solution was prepared by sonicating equimolar amounts of sucrose and lithium hydroxide in DMF at room temperature, also for 90 min (see Scheme 1).

Table 1. XPS elemental analysis data (at.%) for fluorinated and sucrose functionalized carbon nanostructures

Compound	C1s	F1s	O1s
F-SWCNT	62.6	35.7	1.7
Suc-SWCNT	70.1	18.4	11.5
F-ND	79.1	14.0	5.1
Suc-ND	81.6	12.7	5.7
F-NO	55.7	44.2	0.1
Suc-NO	73.5	21.8	4.7

In a final step, the two solutions were combined into one flask and sonicated at room temperature for another 90 minutes to initiate the reaction between fluorinated carbon nanostructures and LiOR (see Scheme 1). Optimum results were obtained at a 5 : 1 molar ratio of LiOR to fluorinated carbon material. After the reaction completion, the end products, Suc-SWCNT and Suc-NO, were collected on a Teflon membrane (pore size 0.2 μm) by filtration. In the case of Suc-NDs, first the solvent (DMF) was removed *in vacuo* at 50 °C using a rotary evaporator, the solid residue was dissolved in water, and the soluton was filtered through a polycarbonate membrane (pore size 0.05 μm). Suc-NDs in the form of finely dispersed powder was precipitated onto the menbrane. All products were washed with large amounts of water to assure complete removal of nonbonded sucrose and then dried overnight in a vacuum dessicator at room temperature.

The epoxy derivatization of Suc-SWCNTs yielding Epoxy-SWCNT product was carried out by dispersing 50 mg of Suc-SWCNTs in 200 mL of anhydrous acetone, adding 12 mg of 4,4′-methylenebis(phenylisocyanate), and stirring the mixture at room temperature for 24 h. Then, 10 mg of glycidol (Scheme 2) was added and the mixture was stirred for an

Scheme 2

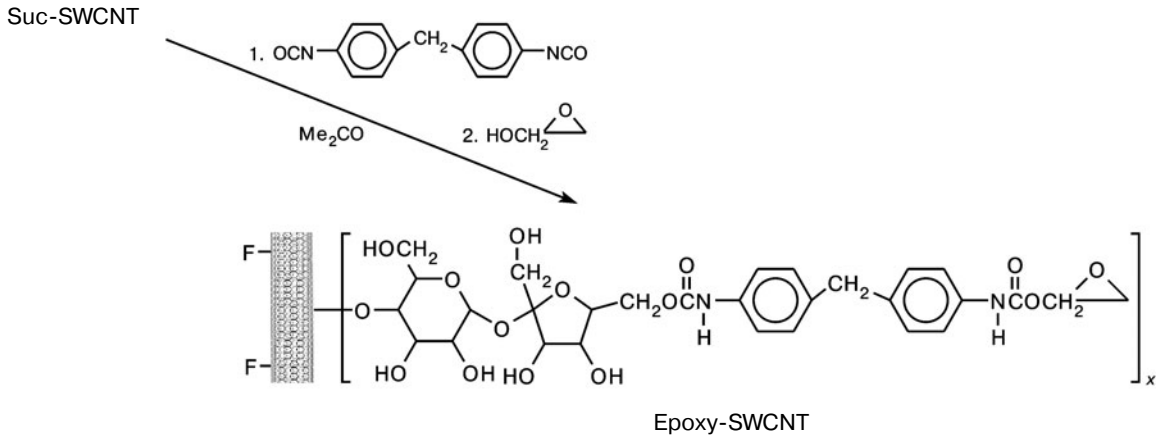

Epoxy-SWCNT

additional 24 h. An Epoxy-SWCNT product was formed and precipitated onto a Teflon membrane (pore size 0.2 μm) during filtration of the mixture.

The fluorinated and sucrose functionalized SWCNT, NO, and ND materials were characterized by FTIR, Raman, and UV—Vis spectroscopies, XPS, TGA-DTA, scanning electron (SEM), transmission electron (TEM), and atomic force (AFM) microscopies. The FTIR spectral measurements were performed using a Thermo Nicolet Nexus 670 FTIR Spectrometer. The transmission mode FTIR spectra were collected from samples pressed into KBr pellets.

The Raman spectra were collected with a Renishaw 1000 Microraman System operating with 514-nm and 780 nm laser sources. UV—Vis spectra were obtained using a Cary 5000 UV—Vis—NIR spectrophotometer. Thermal analysis was done with a TA-SDT-2960 TGA-DTA analyzer by heating samples in a platinum pan from room temperature to 800 °C in an argon atmosphere. XPS data were collected with a PHI Quantera X-ray photoelectron spectrometer using a monochromatic Al-Kα radiation source with a power setting of 95.4 W and an analyzer pass energy of 26 eV. To examine the surface morphology, SEM was performed on a FEI Quanta 400 ESEM FEG instrument at 30 kV beam energy in high vacuum mode. TEM images were obtained using a JEOL JEM-2010 electron microscope operating at an accelerating voltage of 100 kV. AFM analysis was done with a Nanoscope IIIA AFM equipped with a Silicon tip.

Results and Discussion

Sucrose Functionalization of Nanocarbons. Sucrose is a non-reducing disaccharide, and for that reason is considered relatively stable toward alkali-catalyzed degradation proceeding very slowly at ambient temperatures. Earlier studies have shown that treatment of sucrose solutions with concentrated alkali hydroxides produces soluble monosubstituted metal sucrates, unlike reactions of sucrose with alkali earth and other metal bases, which can yield polysubstituted products.[24] More recent works[25,26] have found that the alkaline substitution takes place at the most acidic proton of the hydroxyl group, which is attached to the C(1′) atom of the fructose ring in the sucrose. In view of these studies it was reasonable to assume that our treatment of the sucrose solution in DMF by LiOH under sonication at room temperature yielded a lithium monosucrate LiOR product according to Scheme 1.

The obtained solution of LiOR showed no color, unlike the intense brown-colored products observed to appear in refluxed water solutions (100 °C) of sucrose in the presence of alkali due to degradation of sucrose.[25,27] The subsequent reactions of LiOR with F-SWCNTs, F-NOs, and F-NDs (see Scheme 1) were also carried out in DMF since these fluorinated nanocarbons are soluble in DMF.[7,13–16] The final products, Suc-SWCNTs and Suc-NOs, were isolated from DMF solutions by straightforward precipitation on a Teflon filter membrane (pore size 0.2 μm). The separation of much smaller sized Suc-ND nanoparticles was done after the solvent was first evaporated *in vacuo* and then the solid residue obtained was washed with water on a polycarbonate membrane (pore size 0.05 μm). Since evaporation of DMF required heating at 50 °C, the batch solution was observed to turn light-yellow, indicating that some degree of alkali-induced degradation of sucrose groups in Suc-NDs could possibly take place.

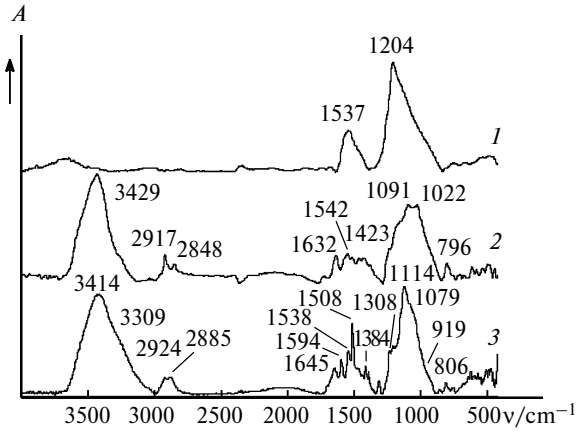

Fig. 1. FTIR spectra of functionalized carbon nanotubes: F-SWCNT (*1*), Suc-SWCNT (*2*), and Epoxy-SWCNT (*3*).

FTIR spectroscopy. The FTIR spectra provide structural information on the functional groups present on the surface of carbon nanoparticles before and after the derivatization reaction. In the spectrum of the F-SWCNT sample (Fig. 1), the absorption band of the C—F stretch shows at 1204 cm^{-1}, while the band of activated sidewall C=C stretches appears near 1537 cm^{-1}, in agreement with the IR characterization data on fluorinated HipCO SWCNTs.[13–15]

In the spectra of Suc-SWCNTs, the strong broad peak at 3429 cm^{-1} corresponds to O—H stretches. The two peaks in the interval 2800—3000 cm^{-1} are due to the C—H stretches of the sucrose functional groups. The small peak at 1632 cm^{-1} is most likely related to moisture absorbed on the hydrophilic surface of Suc-SWCNTs. Peaks observed at 1542 cm^{-1} and in the 1350—1460 cm^{-1} region are related to activated sidewall C=C stretching and sucrose C—H bending motions, respectively. A shoulder peak near 1200 cm^{-1} is most likely due to the C—C stretches, while strong bands at 1091 and 1022 cm^{-1} and a weaker band at 796 cm^{-1} characterize the sucrose C—O stretching modes.[28,29]

The spectrum of fluorinated NOs (Fig. 2, *a*, curve *1*) shows a dominant peak at 1209 cm^{-1}, which belongs to the stretching vibrations of the tertiary C—F bonds[7] formed by covalent addition of fluorine to graphene layers in the NOs. A very weak absorption observed in the spectra at 1574 cm^{-1} is assigned to the vibrational mode of the "fluoroolefinic" C=C bonds in F-NOs which become IR active due to breaking of the aromatic structure of the NO graphene layers through the addition of fluorine. The

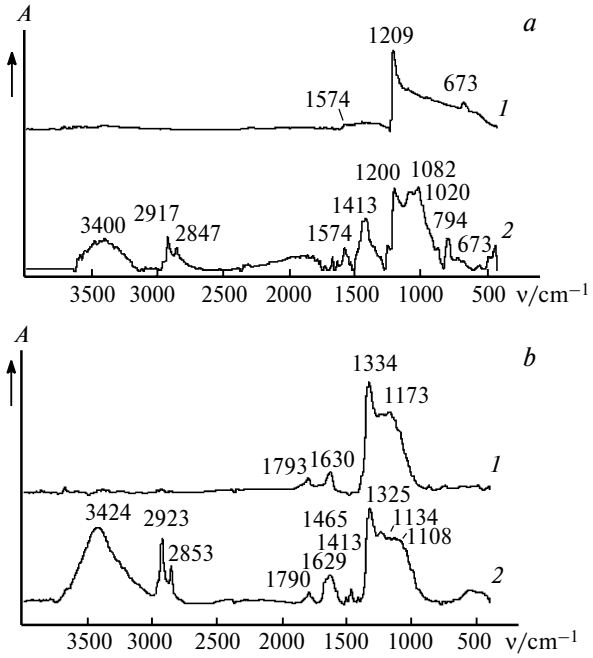

Fig. 2. FTIR spectra of functionalized NO (*a*) and ND (*b*); (*a*) F-NO (*1*) and Suc-NO (*2*); (*b*) F-ND (*1*) and Suc-ND (*2*).

band of the C—F stretch weakens and shifts in the spectrum of Suc-NOs (Fig. 2, *a*, curve *2*) along with the appearance of the peaks characterizing the sucrose moieties[28] at 3400 cm^{-1} (O—H stretch), 2917 and 2847 cm^{-1} (C—H stretch), 1413 cm^{-1} (CH deformation), in the 1200—900 cm^{-1} range and at 794 cm^{-1} (C—C and C—O stretches).

The C—F stretches in the spectrum of F-NDs (see Fig. 2, *b*, curve *1*) appear in the 1100—1400 cm^{-1} interval,[16] at higher wavenumbers than in the spectra of F-SWCNTs and F-NOs, indicating a stronger C—F bonding at the ND surface. Very weak bands at 1798 and 1630 cm^{-1} belong to residual surface C=O and C=C groups which remain virtually unchanged after transformation of F-NDs into Suc-NDs.

The FTIR spectrum of Suc-NDs (see Fig. 2, *b*, curve *2*) shows the absorptions of sucrose O—H stretching vibrations at 3424 cm^{-1} and C—C and C—O stretches in the 1250—950 cm^{-1} region.[28,29] Also, the figure shows IR peaks of the C-H stretches at 2923 and 2853 cm^{-1} and of the deformation modes at 1465 and 1413 cm^{-1}.

Raman spectroscopy. The Raman spectra (Fig. 3) provide evidence of sidewall functionalization of carbon nanotubes[13a,14,15] by showing a strong increase (with respect to pristine SWCNTs) in intensity of the D-peak near 1300 cm^{-1} which is generally accepted to be due to introduced sp^3 carbon atoms acting as defects required in the underlying double-resonant Raman process.[14a] It is also clear from comparison of the spectra of fluorinated and sucrose functionalized carbon nanotubes (see Fig. 3)

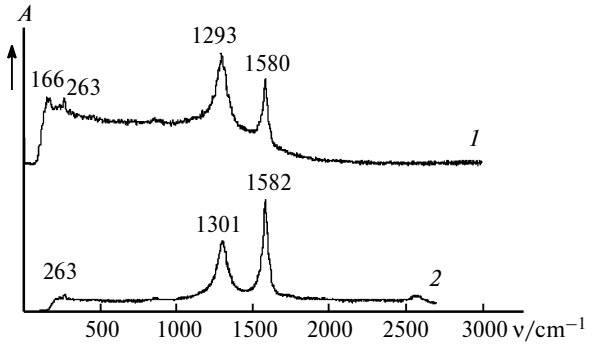

Fig. 3. Raman spectra (λ = 780 nm) of functionalized SWCNTs: F-SWCNTs (*1*) and Suc-SWCNT (*2*).

that fluorine removal and substitution took place during the reaction, resulting in bonding of sucrose molecules to the sidewalls. This is reflected by the decrease in the intensity and a shift of the D-peak from 1293 cm^{-1} in F-SWCNTs to 1301 cm^{-1} in Suc-SWCNTs, and a shift of the G-peak from 1580 cm^{-1} in F-SWCNTs to 1582 cm^{-1} in Suc-SWCNTs.

In contrast, the integrated D/G peak relative intensity in the Raman spectra of Suc-NOs does not change significantly in comparison with F-NOs, aside from slight shifts of the peaks (Fig. 4, *a*). Based on the earlier established fact that F-NOs are structurally built of fluorographene multilayers,[7] the minor changes observed in the Raman spectrum of Suc-NOs can be explained by the substitution of fluorine by sucrose taking place only at the external surface layer in F-NOs while the internal fluorinated layers remain intact.

The Raman spectrum of fluoro-nanodiamond is similar to that of pristine nanocrystalline diamond powder, showing two broad peaks at 1324 and 1630 cm^{-1} (Fig. 4, *b*) which are slightly shifted from the 1326 and 1625 cm^{-1} peaks observed for NDs.[30–32] The first band is typical of a nanosized diamond consisting of small atomic clusters of ordered sp^3-bonded carbon. The second band at 1625—1630 cm^{-1} indicates the presence of weakly ordered clusters of sp^2-bonded carbons considered both as an impurity in the initial powder and partly as a constituent of the outer shells of nanoparticles creating bonded sp^2/sp^3 state carbons so that not only aromatic but also isolated C=C double bonds are present on ND and F-ND surfaces.[30,31]

In comparison with the F-NDs, in the Raman spectrum of Suc-NDs (see Fig. 4, *b*) two new stronger peaks at 1139 and 1517—1530 cm^{-1} are found in addition to weaker "nanodiamond peaks" at 1327 and 1635 cm^{-1}. These new peaks are not detected in the Raman spectra of Suc-SWCNTs and Suc-NOs, synthesized under the same conditions as Suc-NDs (see Experimental).

By taking into consideration the possibility of LiOH mediated partial degradation of the sucrose structure in

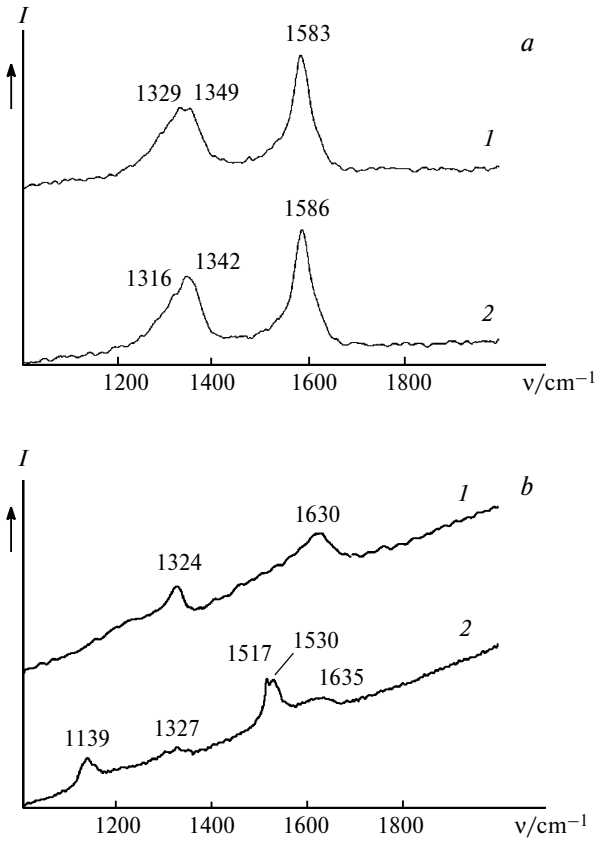

Fig. 4. Raman spectra (λ = 514 nm) of functionalized NO (*a*) and ND (*b*); (*a*) F-NO (*1*), Suc-NO (*2*); (*b*) F-ND (*1*), Suc-ND (*2*).

Suc-NDs in the course of removal of DMF solvent from the reaction batch on the rotary evaporator, these bands can be attributed to vibrations of HC=C—O units formed in the fructose or glucose rings of the sucrose structure during the secondary reactions.[25]

TGA-DTA studies. These studies present further verification of covalent derivatization of carbon nanostructures by sucrose molecules. The TGA-DTA plots for all sucrose-functionalized samples (Fig. 5) show a weight loss in the temperature interval 200–350 °C. This is due to sucrose that detaches from the surface of the functionalized nanostructures and undergoes thermal degradation. The weight loss at temperatures above 400 °C is associated with removal of the residual fluorine from the surface of the fluorinated and derivatized carbon nanoparticles in the form of CF_4.[13–16] Sucrose functionalized SWCNTs exhibit the largest weight loss (Fig. 5, *a*). This fact can be explained by a higher reactivity of fluorinated nanotubes in comparison with the F-NDs (see Fig. 5, *b*) and F-NOs (see Fig. 5, *c*) and also by the fact that the internal carbon layers in the latter two nanostructures remain intact and thus do not contribute to weight loss during TGA. From the weight loss data, the degree of

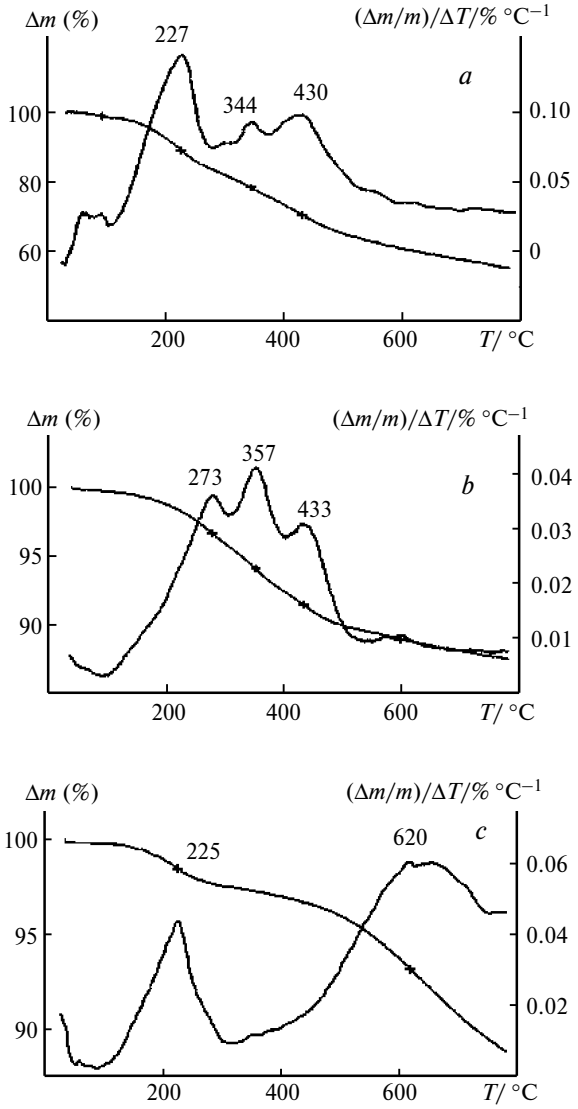

Fig. 5. TGA-DTA plots for sucrose functionalized nanocarbon mayerials: Suc-SWCNT (*a*), Suc-NO (*b*), and Suc-ND (*c*).

sidewall functionalization by sucrose in Suc-SWCNTs was calculated to be 1 in 42 carbons.

XPS Analysis. The results of XPS surface analysis, which usually provides sampling at only a few nanometers depth from the solid surface, showed carbon, fluorine, and oxygen peaks for all samples. The elemental analysis data are summarized in Table 1.

The high-resolution XPS C1s spectra of sucrose functionalized SWCNTs, NOs, and NDs are shown in Figure 6. These data provide information on the extent of fluorine removal from F-SWCNTs, F-NOs, and F-NDs both through displacement by sucrose and defluorination reactions. All fluorinated nanocarbons have shown a reduced fluorine content after reactions with lithium sucrate LiOR. The most notable reduction in the fluorine content was found for Suc-SWCNT and Suc-NO deriva-

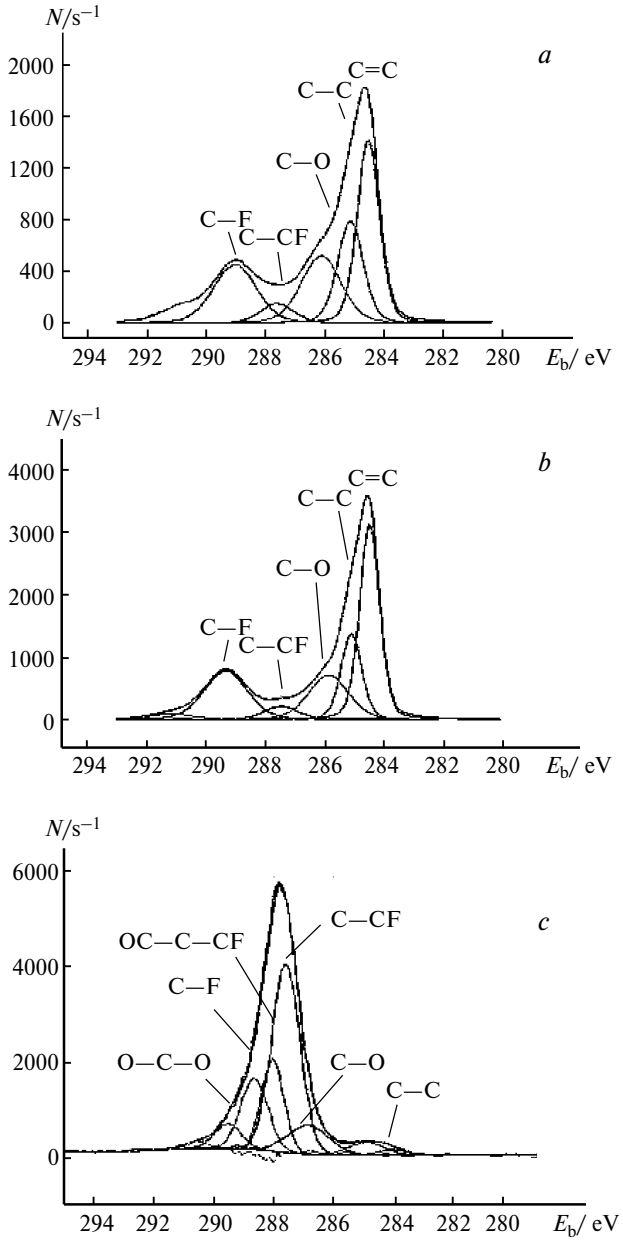

Fig. 6. Curve-fitting analysis of C1s peaks in the XPS spectra of sucrose functionalized carbon nanomaterials: Suc-SWCNT (*a*), Suc-NO (*b*), and Suc-ND (*c*); *N* is the number of events per second.

tives, from 35.7 to 18.4 at.%, and 44.2 to 21.8 at.%, respectively, while for Suc-NDs, the extent of fluorine content reduction was found to be much smaller, from 14.0 to 12.7 at.% (Table 1), indicating a lower reactivity of the C—F bond in F-NDs than in F-SWCNTs and F-NOs.

The high-resolution XPS C1s spectra of functionalized graphene-type nanostructures, Suc-SWCNTs and Suc-NOs (Fig. 6, *a*, *b*), are quite similar, each showing after a curve-fitting analysis the peaks at 284.5, 285.0—285.1, 286.0—286.2, 287.6, and 289.0—289.3 eV due to the C=C, C—C, C—O, C—CF, and C—F bonded carbons, respectively. Although the peaks found through a curve-fitting in the C1s spectrum of Suc-NDs (see Fig. 6, *c*) appear at positions close to those in the spectra of Suc-SWCNTs and Suc-NOs, they show significantly different relative intensities. For instance, the peak at 284.2 eV shows a very low intensity and most likely characterizes the sp^2 carbons from the C=C bonds formed during partial thermal degradation of sucrose groups. The most intense peaks in this spectrum (see Fig. 6, *c*), at 287.4, 287.9, and 288.5 eV, are due to the sp^3 carbons located in different bonding environments, such as C—CF, OC—C—CF, and C—F, respectively. The less intense peaks at 285.0, 286.9, and 289.5 eV characterize the sucrose group carbons of the C—C, C—O, and O—C—O units.

Microscopy analysis. Our previous studies of covalently functionalized carbon nanostructures by microscopy methods have shown that the combination of SEM, TEM, and AFM can provide the most informative data in support of occurrence of surface functionalization when applied to functionalized SWCNTs.[7,13–20] The microscopy data, obtained for sucrose-functionalized SWCNTs are shown in Fig. 7. According to the SEM image (see Fig. 7, *a*), the surface morphology and the extent of nanotube bundling of Suc-SWCNTs within bulk nanotube samples are different from the pristine and fluorinated SWCNTs.[13–15,19] The presence of sucrose on the SWCNT surface facilitates aggregation of Suc-SWCNTs through the hydrogen bonds formed by hydroxyl groups. Such aggregates appear like a cellulose wool in the SEM image (see Fig. 7, *a*).

The TEM and AFM images (see Fig. 7) provide direct evidences of covalent functionalization of SWCNTs. The TEM image (Fig. 7, *b*) clearly shows very thin bundles of Suc-SWCNTs which are surface-modified. The sucrose molecules attached to the nanotube sidewalls appear as buds or short twigs. The AFM image of the specimen from Suc-SWCNTs (see Fig. 7, *c*) shows coating on the backbones of nanotubes. From the cross-section height analysis indicated by the flags in Fig. 7, *d* the size of the individual nanotubes with sidewall-attached molecules was estimated to be 2.573 nm. This value reasonably agrees with the sum of the average F-SWCNT diameter (about 1.3 nm) and approximate size of a sucrose molecule (~1.0—1.3 nm).

Solubility. It is always regarded that pristine carbon nanostructures, as well as their fluorinated derivatives, are insoluble in water.[1,13–15] By contrast, our results show that all sucrose-functionalized nanocarbons prepared in this work are soluble in water and other polar solvents. The photographs of water suspensions taken after sonication followed by one week standing are shown in Fig. 8. The fluorinated nanocarbons, due to their hydrophobic nature, do not disperse and remain on top of water, while the samples functionalized with the highly hydrophilic sucrose form either dark (Suc-SWCNTs and

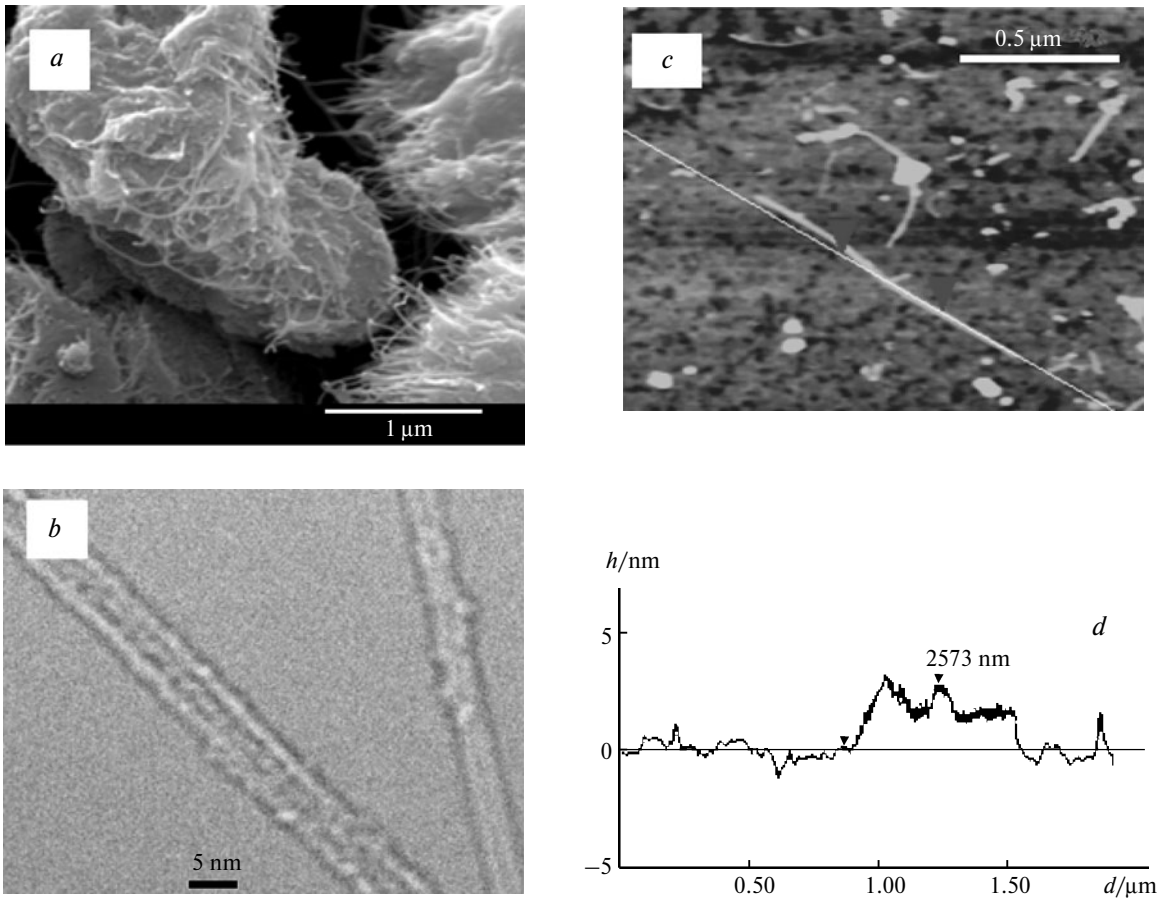

Fig. 7. Microscopy data on sucrose-functionalized SWCNT samples: a SEM image (*a*); a high-resolution TEM image of very thin bundles consisting of three (left) and two (right) sucrose functionalized nanotubes (*b*); an AFM image showing several individual nanotubes having different lengths (*c*); nanotube height measurement profile obtained by section analysis run along the backbone of individual Suc-SWCNT shown in Fig. 7, *c* (*d*).

Suc-NOs) or light-yellow (Suc-NDs) solutions. It should be noted that the addition of only a small amounts of 2 *M* HCl followed by 1 h sonication causes complete precipitation of water-solubilized nanocarbons due to cleavage of sucrose groups, which is known to occur under acidic conditions.[29]

The quantitative estimation of the solvation of functionalized SWCNTs, NOs, and NDs was performed by dispersion (through 1h sonication) of 25 mg sucrose-functionalized carbon nanomaterial in 50 mL of selected solvents (water, ethanol, and DMF). The dispersions were left standing for 7 days. Then the top 40 mL of each solution were decanted and the solid residues in the rest of the solutions were collected by filtration through the membrane, dried *in vacuo* overnight, and then weighed. The solubility data (mg L^{-1}) obtained are presented in Table 2. They show that the sucrose-functionalized sphere-shaped nanocarbons, such as Suc-NOs and Suc-NDs, are about twice as much soluble as one-dimensional tubular nanocarbons (Suc-SWCNTs) in all

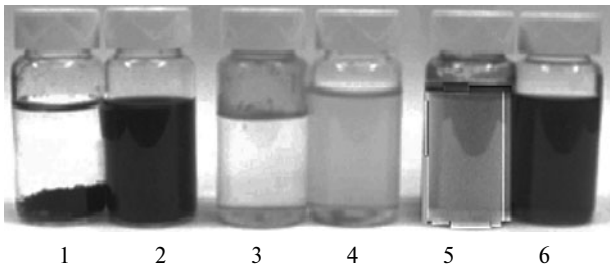

Fig. 8. Photograph of water dispersions of pristine and sucrose functionalized nanocarbons: SWCNT (*1*), Suc-SWCNT (*2*), ND (*3*), Suc-ND (*4*), NO (*5*), and Suc-NO (*6*).

Table 2. Solubility (mg L^{-1}) of sucrose-functionalized SWCNT, NO, and ND in water, ethanol, and DMF

Compound	Water	Ethanol	DMF
Suc-SWCNT	100	110	140
Suc-NO	200	220	400
Suc-ND	180	190	360

three polar solvents tested. Also, the lower density of hollow spheres facilitates the overall best solubility of Suc-NO nanocarbon material.

UV—Vis spectroscopy. The solubility of sucrose-functionalized nanocarbons enables their characterization by UV—Vis spectroscopy, which serves as a probe for the effect of functionalization on surface electronic configuration. In the case of SWCNTs and nano-onions, the covalently attached fluorine and sucrose functional groups can transform the nanocarbon surface from π-bonded polyaromatic structures into polyene structures, while for the σ-type bonded nanodiamond a much smaller change is expected. The UV—Vis spectra of sucrose functionalized nanocarbons dispersed in water are shown in Fig. 9. The spectra of Suc-SWNTs (see Fig. 9, *a*) and Suc-NOs (see Fig. 9, *b*) show single absorption peaks at 255 and 263 nm, respectively, characteristic of π—π* electron transition in the polyaromatic system of curved graphene layers. The absence of additional peaks in the 200—220 nm region, related to π—π* electron transitions in the polyene-type structures and exhibited by F-NOs in particular,[7] is most likely due to a larger extent of surface defluorination and restoration of aromatic structure than substitution of fluorine (see Scheme 1). In comparison with the spectra of graphene-type Suc-SWCNT and Suc-NO samples, the UV—Vis spectrum of an aqueous solution of Suc-ND (see Fig. 9, *c*) was clear of any absorption bands in the 200—1100 nm region.

Derivatization of Suc-SWCNTs. The presence of terminal hydroxyl groups on sucrose molecules covalently bonded to nanocarbons provides opportunity for further chemical derivatization tailored for specific applications. In this work, Suc-SWCNTs were chosen as an example for demonstration of the derivatization route for producing the sidewall functionalized SWCNTs with the terminal epoxy groups which were expected to enable dispersion and integration of SWCNTs into an epoxy polymer.[33] This derivatization (see Scheme 2) was carried out through subsequent coupling reactions of Suc-SWCNTs with 4,4′-methylenebis(phenylisocyanate) (step 1) and glycidol (step 2), both proceeding at room temperature. The final product, Epoxy-SWCNT (see Scheme 2), was characterized by FTIR spectroscopy and tested for solubility in water and dispersion in EPON 862/W Cure epoxy polymer system. The IR spectrum of the Epoxy-SWCNT sample (see Fig. 1) shows a broad band in the region 3000—3600 cm^{-1} with the peak at 3414 cm^{-1} (O—H stretch) and a distinct shoulder at 3309 cm^{-1} (N—H stretch of the amide group) which is overlapping the weaker bands of the C—H stretches of phenyl and glycidyl groups in the 3000—3100 cm^{-1} region. Bands at 1645, 1538, and 1508 cm^{-1} characterize the C=O stretch and N—H bending modes of the C(=O)NH amide units, while the peak at 1594 cm^{-1} can be related to the aromatic C=C stretches in the Epoxy-SWCNT structure (see Scheme 2). The low and

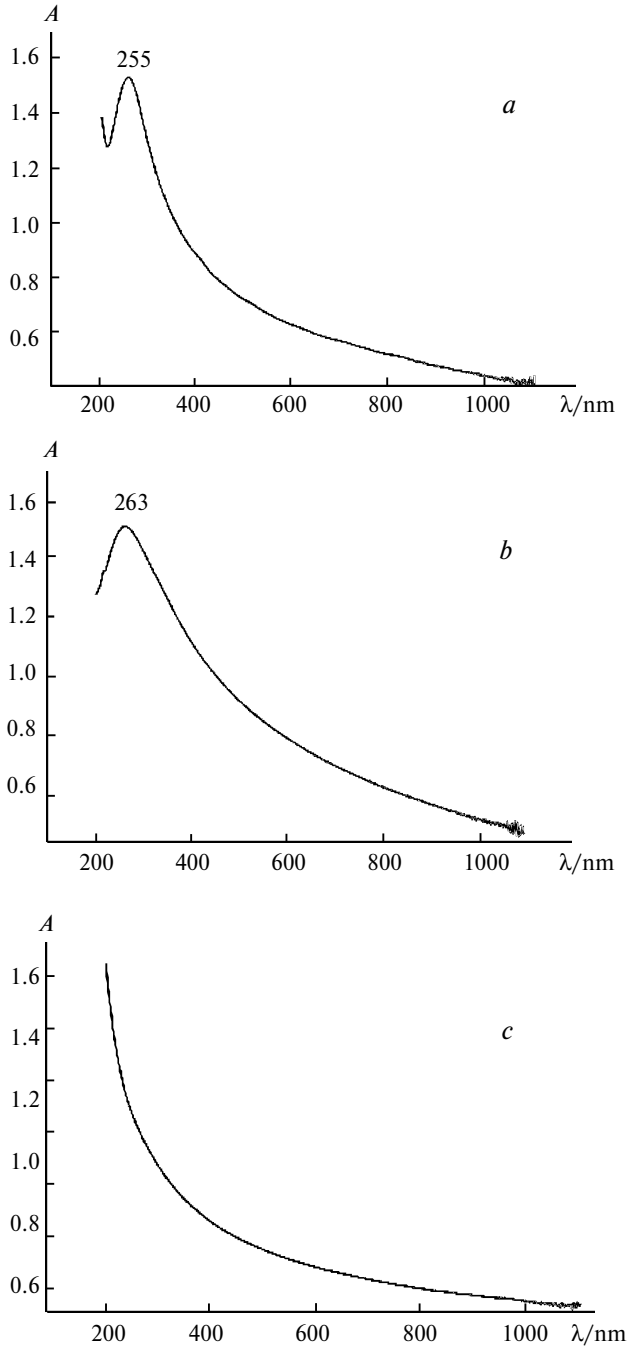

Fig. 9. UV spectra of sucrose functionalized nanocarbons dispersed in water: Suc-SWCNT (*a*), Suc-NO (*b*), and Suc-ND (*c*).

medium intensity peaks in the 1100—1400 cm^{-1} region are due to the deformation and bending modes of the CH_2 and CH of sucrose, glycidyl, and aromatic units.[34] The absorptions due to the C—O stretches in the sucrose and epoxy rings can be associated with a shoulder band observed at 1079 cm^{-1} and weaker bands at 919, 851, and 806 cm^{-1}.

Unlike Suc-SWCNTs, the Epoxy-SWCNT derivative does not form stable suspension solutions in water, show-

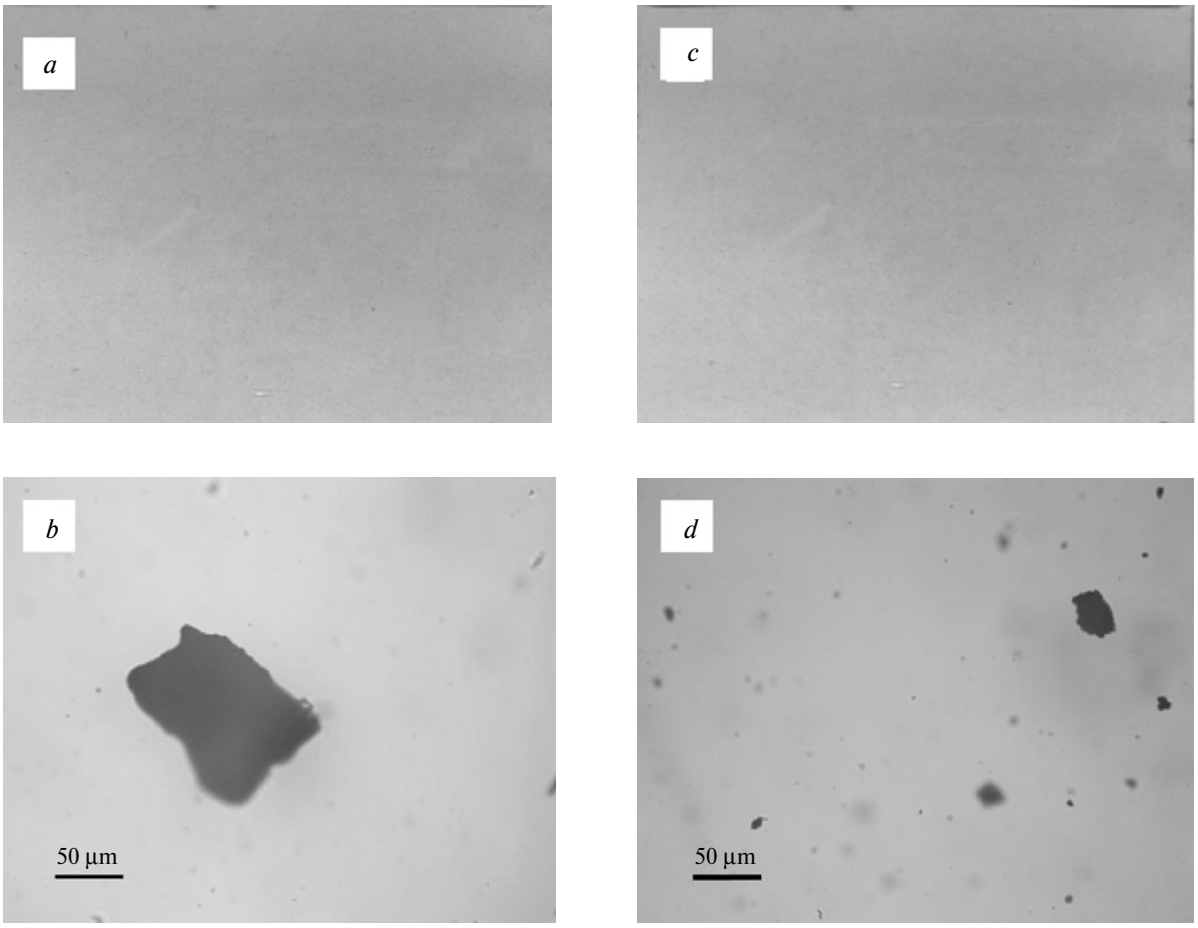

Fig. 10. Dispersions of 0.015 wt. % Suc-SWCNT and Epoxy-SWCNT in EPON 862/W Cure epoxy system: Suc-SWCNT (*a*, *b*) and Epoxy-SWCNT (*c*, *d*); photographs (*a*, *c*) and optical microscope 20X images (*b*, *d*) taken after curing of the samples.

ing complete precipitation just after overnight standing. Nevertheless, these functionalized SWCNT derivatives both show a quite uniform dispersions of their 0.015 wt.% loadings into EPON 862/W Cure epoxy polymer system, demonstrated by the photographs taken from samples cured in a borosilicate glass mold (Fig. 10). Optical microscope images taken on the same samples at 20X magnification, however, revealed the presence of Epoxy-SWCNT nanotube agglomerates which are much smaller than those of Suc-SWCNTs, indicating a higher degree of debundling of Epoxy-SWCNTs and stronger interfacial interaction with the epoxy polymer. This should lead to enhancement of mechanical properties of epoxy composites processed with Epoxy-SWCNTs. Work on processing, fabrication, and testing this type of composites is in progress.

We have demonstrated an efficient one-step method for covalent surface modification of fluorinated SWCNTs, carbon nano-onions, and nanodiamond particles with sucrose molecules. Covalent bonding has been confirmed by the use of several techniques of material characterization that showed that the local environment of the fluorine atoms has been modified through this newly developed functionalization method. The sucrose functionalized nanomaterials obtained are soluble in water and are supposed to be biocompatible nanostructures. This improved property will facilitate applications of sucrose-functionalized nanocarbons in nanomedicine and biology. Subsequent derivatization of hydroxyl groups in sucrose functional moieties creates an opportunity for tailoring the nanocarbons to specific applications in composites, coatings and sensors. Further functionalization reactions and corresponding properties of functionalized nanocarbons are being investigated.

This project was carried out under support through Awards N RUE 2-2659-MO-05 and N RUE2-2894-TI-07 from the US Civilian Research and Development Foundation for Independent States of Former Soviet Union (CRDF), NASA-Johnson Space Center (Grant NNX07AL50G), and the Ministry of Science and Education of Portugal (MCTES — sabbatical grant).

References

1. (a) E. G. Rakov, *Russ. Chem. Revs*, 2001, **70**, 827; (b) A. Hirsch, *Angew. Chem., Int. Ed.*, 2002, **41**, 1853; (c) A. Hirsh, O. Vostrowsky, *Top. Curr. Chem.*, 2005, **245**, 193.
2. S. Banerjee, T. Hemraj-Benny, S. S. Wong, *Adv. Mater.*, 2005, **17**, 17.
3. Y. Show, M. A. Witek, P. Sonthalia, G. M. Swain, *Chem. Mater.*, 2003, **15**, 879.
4. E. Wilks, J. Wilks, *Properties and Applications of Diamond*, Butterworth, Oxford, England, 1997.
5. M. Choi, I. S. Altman, Y. J. Kim, P. V. Pikhitsa, S. Lee, G. S. Park, T. Jeong, J. B. Yoo, *Adv. Mater.*, 2004, **16**, 1721.
6. J. C. Francis, *Solid Lubricants and Self-lubricating Solids*, Academic Press, New York, 1972.
7. Y. Liu, R. L. Vander Wal, V. N. Khabashesku, *Chem. Mater.*, 2007, **19**, 778.
8. A. Bianco, K. Kostarelos, C. D. Partidos, M. Prato, *Chem. Commun.*, 2005, 571.
9. A. S. Rettenbacher, B. Elliott, J. S. Hudson, A. Amirkhanian, L. Echegoyen, *Chem. Eur. J.*, 2005, **12**, 376.
10. A. Krüger, Y. Liang, G. Jarre, J. J. Stegk, *Mater. Chem.*, 2006, **16**, 2322.
11. J. J. Stephenson, J. L. Hudson, A. D. Leonard, B. K. Price, J. M. Tour, *Chem. Mater.*, 2007, **19**, 3491.
12. L. Feng, J. M. Beach, P. K. Rai, W. Guo, R. H. Hauge, M. Pasquali, R. E. Smally, W. E. Billups, *Chem. Mater.*, 2006, **18**, 1520.
13. (a) V. N. Khabashesku, W. E. Billups, J. L. Margrave, *Acc. Chem. Res.*, 2002, **35**, 1087; (b) Y. S. Lee, T. H. Cho, B. K. Lee, J. S. Rho, K. H. An, Y. H. Lee, *J. Fluorine Chem.*, 2003, **120**, 99; (c) A. V. Krestinin, A. P. Kharitonov, Yu. M. Shul´ga, O. M. Zhigalina, E. I. Knerel´man, M. Dubois, M. M. Brzhezinskaya, A. S. Vinogradov, A. B. Preobrazhenskii, G. I. Zvereva, M. B. Kislov, V. M. Martynenko, I. I. Korobov, G. I. Davydova, V. G. Zhigalina, N. A. Kiselev, *Nanotechnologies in Russia*, 2009, **4**, 115.
14. (a) M. Burghard, *Surface Sci. Reports*, 2005, **58**, 1; (b) V. N. Khabashesku, M. X. Pulikkathara, *Mendeleev Commun.*, 2006, 61.
15. (a) V. N. Khabashesku, *Fluorination of Carbon Nanotubes*, in *Chemistry of Carbon Nanotubes*, Eds V. A. Basiuk, E. A. Basiuk, Stevenson Ranch, CA: ASP Publishers, 2007, Vol. **1**, 522; (b) V. N. Khabashesku, O. V. Kuznetsov, M. X. Pulikkathara, *Carbon Nanotubes: Fluorinated Derivatives in Nanomaterials: Inorganic and Bioinorganic Perspectives*, Eds C. M. Lukehart, R. A. Scott, John Wiley and Sons, Ltd, Chichester, 2009, 856 pp.
16. Y. Liu, Z. Gu, J. L. Margrave, V. N. Khabashesku, *Chem. Mater.*, 2004, **16**, 3924.
17. V. N. Khabashesku, H. Peng, J. L. Margrave, *Nanotube-Amino acids and Methods for Preparing Same* (WO/2005/070828), Internat. Pat. Application No.: PCT/US2005/001310, Internat. Filing Date: 18.01.200, Priority Data: 60/537,982 21.01.2004 US.
18. M. X. Pulikkatara, V. N. Khabashesku, *Izv. Akad. Nauk. Ser. Khim.*, 2008, 1035 [*Russ. Chem. Bull., Int. Ed.*, 2008, **57**, 1054].
19. M. X. Pulikkathara, O. V. Kuznetsov, V. N. Khabashesku, *Chem. Mater.*, 2008, **20**, 2685.
20. L. Zhang, V. U. Kiny, H. Peng, R. F. M. Lobo, J. L. Margrave, V. N. Khabashesku, *Chem. Mater.*, 2004, **16**, 2055.
21. S. J. V. Frankland, A. Caglar, D. W. Brenner, M. J. Griebel, *J. Phys. Chem. B*, 2002, **106**, 3046.
22. J. N. Coleman, U. Khan, Y. K. Gun´ko, *Adv. Mater.*, 2006, **18**, 689.
23. (a) P. Nikolaev, M. J. Bronikowski, R. K. Bradley, F. Rohmund, D. T. Colbert, K. A. Smith, R. E. Smalley, *Chem. Phys. Lett.*, 1999, **313**, 91; (b) R. L. Vander Wal, A. J. Tomasek, K. W. Street, D. R. Hull, W. K. Thompson, *Appl. Spectrosc.*, 2004, **58**, 230.
24. C. A. Browne, *A Handbook of Sugar Analysis*, John Wiley and Sons, New York; Chapman and Hall, London, 1912, p. 676.
25. M. Manley-Harris, W. Moody, G. N. Richards, *Austral. J. Chem.*, 1980, **33**, 1041.
26. J. Fitremann, Y. Queneau, J.-P. Maitre, A. Bouchu, *Tetrahedron Lett.*, 2007, **48**, 4111.
27. P. E. Shaw, J. H. Tatum, R. E. Berry, *J. Agr. Food. Chem.*, 1969, **17**, 907.
28. P. L. Polavarapu, S. R. Chatterjee, D. F. Michalska, *Carbohydrate Res.*, 1985, **137**, 253.
29. M. V. Korolevich, R. G. Zhbankov, V. V. Sivchik, *J. Mol. Struct.*, 1990, **220**, 301.
30. J. W. Ager III, D. K. Veirs, G. M. Rosenblatt, *Phys. Rev. B*, 1991, **43**, 6491.
31. A. C. Ferrari, J. Robertson, *Phys. Rev. B*, 2000, **61**, 14095.
32. V. A. Davydov, A. V. Rakhmanina, S. Rols, V. Agafonov, M. X. Pulikkathara, R. L. Vander Wal, *J. Phys. Chem. C*, 2007, **111**, 12918.
33. S. Wang, R. Liang, B. Wang, C. Zhang, *Nanotechnology*, 2008, **19**, 085710.
34. N. P. G. Roeges, *Guide to the Complete Interpretation of Infrared Spectra of Organic Structures*, Jonn Wiley and Sons Publ., Chichester—New York—Brisbane—Toronto—Singapore, 1994.

Received November 27, 2008;
in revised form November 24, 2009